9. National Conference on Computational Mechanics
MekIT'17
B. Skallerud and H I Andersson (Eds)

MULTIPHASE FLOW SIMULATION IN AN ANNULUS CONFIGURATION

Christopher J. Friedemann[1], Mikael Mortensen[1] and Jan Nossen[2]

[1]Department of Mathematics
University of Oslo
Nils Henrik Abels hus, 0851 Oslo, Norway
e-mail: postmottak@mn.uio.no, web page: http://www.mn.uio.no

[2] Institute for Energy Technology (IFE)
Oil and Gas
Instituttveien 18, 2007 Kjeller, Norway
e-mail:firmapost@ife.no, web page: https://www.ife.no/en

Key words: CFD,Multiphase, OpenFOAM,VOF, Concentric annulus

Abstract. In this present study, four multiphase flow cases were simulated in an annulus pipe configuration using the interFoam solver in OpenFOAM. Three of the cases were conducted using a $k-\omega$ RANS model while the remaining simulation was executed with a one equation LES formulation. The annulus consists of two concentric cylinders where the outer diameter is 0.1 m and the inner diameter is 0.05 m. Pipe geometries of lengths between 2 and 10 m were meshed and applied with periodic boundary conditions across the inlet and outlet. A pressure drop was administered throughout the domain of each case with a magnitude between 110 Pa/m and 1157 Pa/m. Additionally the mesh used in the RANS simulation model was constructed with a symmetric boundary condition along xy-plane to reduce the size of the computational mesh. The internal domain was initialized with liquid volume fractions and superficial velocities based on experimental data provided by IFE. The cases yielded wavy flow with indications of a possible transition to slug flow in cases 3 and 4. All cases displayed waves of varying amplitude and frequency. Comparing to experiments conducted at IFE, the high frequency low amplitude flow regime in case 1 matched well in terms of the velocity field. Cases 3 and 4 with larger waves had prevalent discrepancies between the applied pressure drop and expected phase velocity when contrasted to the experimental Results

1 INTRODUCTION

Multiphase pipe flow is most frequently associated with the oil, gas and power industries. That said, it is applicable to a vast range of other fields including aerospace and

medicine. Generally speaking multiphase flow problems consist of two or more separate fluids present in a system. These fluids behave according to their state, physical conditions and properties of the system such as pressure, surface roughness and fluid velocities. When considering an annulus configuration the hydraulic diameter also plays a vital part. The coupling between the phase interaction and pipe geometry further contribute to the complexity of the problem. The accurate prediction of flow pattern, liquid holdup, phase fraction at arrival and pipeline pressure distribution are of immediate concern to oil companies[1, 6]. These concerns consist of several aspects, including pipeline design and maintenance, flow efficiency, safety and preservation of the environment.

There are several empirical models such as the method developed by Beggs et al.[2] and mechanistic models that can be used to predict pipeline behavior. Mechanistic models include the original pioneering work of Taitel et al. [10] which in turn has lead to more recent efforts, one of which is the methods devised by Petalas [8]. Mechanistic models are more robust compared to the empirical counterpart as they are based on fundamental physics. However they too employ said empirical correlations as well as other estimates which contributes to an underlying uncertainty built into the results. Even so, a good mechanistic model is often reasonable enough when employed correctly that it can be used together with well data or experiments to validate a CFD model.

Empirical models are easy to use and readily available from several sources. Although easy to implement they are still only as good as the data from which they are derived and as such should only ever be used for similar cases. Even in cases that are applicable the simplification of the physics involved contribute to a significant uncertainty [11].

Most ready-made models, including empirical, mechanistic and commercial flow simulators are set up to handle multiphase pipe flow in a conventional configuration. Despite the direct relationship with the drilling and well control industries, very little work has been done to categorize flow within an annulus. In industry annulus flow occurs intentionally in the gas-filled compartment of a gas-lifted well [6], and unintentionally in the drilling industry during a blow-out. Considering how important annulus multiphase flow is in the industry, it comes as a surprise that there is a serious lack of dedicated research to the topic. Perhaps the lack of concern can be attributed to the fact that prior to the Deepwater Horizon Oil spill in 2010 no incident had occurred which warranted extensive research.

After the 2010 oil spill regular multiphase flow models were used to estimate the oil spill based on the frequency of slugs at the site. However questions should be raised about the approach of applying these methods to an annulus. Considering that the encased cylinder drastically alters the behavior of the flow within, it affects the hydraulic diameter, the friction factor, the interfacial area between the fluids and so on. At the time of the Deepwater horizon incident there were but a few published papers which dealt with any form of multiphase flow in an annulus such as the Caetano[3] thesis in 1985 and Ekberg's[4] paper in 1999, this lack of information somewhat explains why the standard models were used, but not why it was accepted.

Taking into account the lack of experimental studies conducted using an annulus, it was as expected that even less research has been conducted using CFD. It is, after all, very difficult to validate a CFD model without any experimental or field data to compare with.

In this paper an initial attempt at performing CFD simulation using the OpenFOAM solver interFoam on a multiphase annulus problem has been carried out. The simulations will eventually be compared with extensive experiments performed at IFE Kjeller where an ongoing campaign is being conducted and scheduled to run through 2018. The data is available as part of this research project and by utilizing simulations together with the experimental work it nurtures an excellent possibility of expanding the current knowledge base of multiphase flow in the annulus configuration.The two turbulence models used are the Smagorinsky sub grid model for the LES simulation and the k-ω RANS model. The k-ω model has previously been implemented in RANS simulations by Shuard[9] while Peters[7] successfully utilized the Smagorinsky model for his LES simulations in his thesis. As this project is in its infancy these models were chosen as a suitable starting point.

1.1 interFoam Solver

The solver used in this paper was the interFoam solver. This solution method accepts a variety of LES and RANS turbulence models, and can easily be manipulated for different setups. What is important to mention is that the "Volume of Fluid" (VOF) method, which interFoam utilizes, solves the continuity and momentum equations as though the fluids were one. This differs from other possible solvers such as multiphaseEulerFoam which calculates the momentum equations for each phase separately. The VOF method models the flow by solving the momentum equation for the two fluids as if they were a homogeneous mixture, thus density and velocity are averaged and the averaged continuity equation becomes

$$\nabla \cdot \bar{u} = 0, \tag{1}$$

where $\bar{u}$ is the averaged velocity of the two phases such that

$$\bar{u} = \alpha_g u_g + \alpha_l u_l. \tag{2}$$

The subscripts l and g, signify liquid and gas, while α is the phase fraction. Applying them to the momentum equation, while using a similar approach to Eq. 2 for other mixture properties such as density and viscosity yields the momentum equation as

$$\frac{D\bar{u}}{Dt} = -\frac{1}{\bar{\rho}}\nabla p + \bar{\nu}_{eff}\nabla \cdot (\nabla \bar{u} + (\nabla \bar{u})^T) + g + \frac{F_s}{\bar{\rho}}. \tag{3}$$

F_s is the surface tension force, g gravity, while the overbar quantities denote averages of the two phase values.

A governing equation is solved for the phase fraction α

$$\frac{D\alpha_l}{Dt} + \nabla \cdot (u_c \alpha_l \alpha_g) = 0. \tag{4}$$

This equation employs interface sharpening in the region where both phases are present by adding an artificial interface velocity u_c, this interface velocity serves only to create a sharper interface between the phases. The magnitude of the velocity depends on the interface sharpening coefficient (C_α), which in case of this work was set between 0.7 and 1. For interface sharpening coefficients of magnitude equal to or less than 1 the interface compression velocity becomes :

$$u_c = C_\alpha |u| \frac{\nabla \alpha_l}{|\nabla \alpha_l|}. \tag{5}$$

2 GEOMETRY, MESH AND BOUNDARY CONDITIONS

The Geometry of the concentric annulus pipe used in these simulations was created in Gmsh. The outer diameter of the pipe is 0.1 m while the inner diameter is 0.05 m. The pipes used are between 2 and 10 m long. While the 10 m pipe consist of approximately 1.5 million cells, the 2 m pipe has 1.55 million cells. The cells are uniformly distributed in the streamwise and circumferential directions while the cells between the two cylinder walls are refined in the near wall regions as seen in Fig.1.

By carefully describing the separation of the grid elements along transfinite lines it was possible to create the entire mesh using only hexahedral elements as seen in Fig. 1. This is advantageous for the VOF method which the interFoam solver uses. Generating the mesh along transfinite lines with hexahedral elements creates uniform cells with little if any skewness. The direct description of the elements makes the Courant Number estimation for simulation purposes straight forward while also simplifying the mapping of the periodic conditions. The mapping is made trivial because the inlet and outlet patches are an exact geometric match.

The model geometry for the RANS simulation cases were further simplified by applying a symmetric boundary condition across the xy-plane. When there is insignificant amounts of crossflow and the RANS turbulence model is used, Shuard[9] determined that the final results from the full and half mesh were the same. Thus the mesh density can be vastly improved while maintaining or reducing the required simulation time. From previous iterations of the simulations presented here it was the observed that the RANS simulations are indeed mirrored about the centerline.

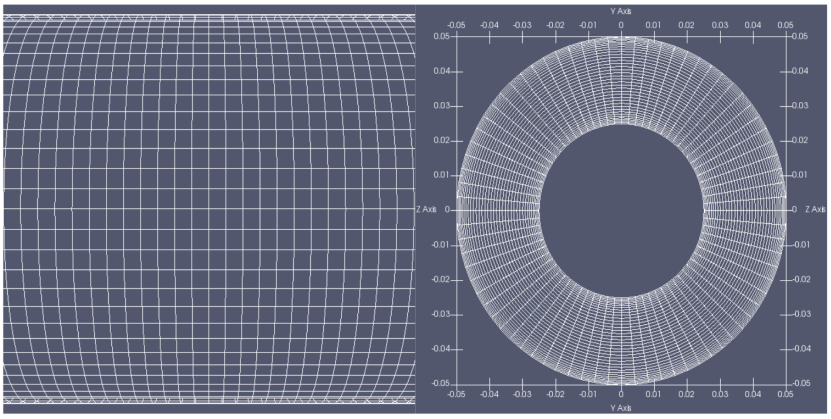

Figure 1: 2 m pipe with 1.55 million cells

After creating the mesh it was converted to the OpenFOAM format. Within the case files of the OpenFOAM framework the boundary conditions and the dynamic solution method was specified.

The initial conditions were chosen by referencing experimental data from IFE, the flow map for multiphase pipe flow by Lee et al.[5] and approximating the superficial phase velocities for the liquid and gas phases in the annulus configuration. The phase velocities, pressure drop, liquid volume fraction and Courant number restrictions for each case are summarized in Table 1. Each case was selected because they are near or at data points provided by IFE and can be compared qualitatively in regards to flow regime and final velocities.

Table 1: Initial conditions

CASE	u_g (m/s)	u_l (m/s)	$\alpha_l(\%)$	$\Delta P(Pa/m)$	CFL_{alpha}	CFL
1	3.24	0.4	22.5	110	0.30	0.40
2	3.23	1.05	38.0	155	0.25	0.40
3	3.24	1.5	43.0	340	0.30	0.40
4	3.0	1.2	38.0	1157	0.30	0.40

In combination with the initial state of the system typical physical properties for oil and gas were chosen to resemble those used in experiments by Nossen et.al[6]. These are summarized in Table 2.

Table 2: physical properties

Phase	viscosity (m^2/s)	density (kg/m^3)	σ
Oil	$2.0 \cdot 10^{-6}$	800.0	0.0285
Gas	$7.56 \cdot 10^{-7}$	24.0	0.0285

As with many computational fluid dynamic problems there are several possible sets of valid boundary conditions or solution methods in OpenFOAM. For this array of simulations periodic inlet and outlet conditions have been used together with a prescribed pressure drop. The standard boundary conditions are summarized in Table 3. Note that, depending on the type of simulation, some of these parameters may not be used. For example, an LES simulation has no need for the omega values and are thus omitted.

Table 3: Boundary Conditions

parameter	inlet	outlet	walls
alpha	Mapped	inletOutlet	zeroGradient
U	Mapped	pressureinletOutletVelocity	noSlip
k	Mapped	inletOutlet	kqRWallFunction
ω	Mapped	inletOutlet	omegaWallFunction
prgh	totalPressure	totalPressure	fixedFluxPressure
ν_T	calculated	calculated	nutkWallFunction

There are several ways of estimating k and ω, for this work a method based on the turbulent intensity and hydraulic diameter was used. The turbulent intensity can be determined by

$$I = 0.16 Re_{d_h}^{-\frac{1}{8}}, \tag{6}$$

where the reynolds number based on the hydraulic diameter is

$$Re_{d_h} = \frac{\bar{u} \cdot d_h}{\bar{\nu}}. \tag{7}$$

The aforementioned averaging procedure based on the phase fraction as seen in Eq. 2 was used to solve for the velocity and viscosity components, while the hydraulic diameter of a concentric pipe is defined as

$$d_h = d_{outer} - d_{inner}. \tag{8}$$

Using Eq. 6-8 the turbulent kinetic energy is solved for by

$$k = \frac{3}{2}(\bar{u}I)^2, \tag{9}$$

after which one can use k to solve for the specific dissipation ω

$$\omega = \frac{C_\mu^{-\frac{1}{4}} k^{\frac{1}{2}}}{l}. \tag{10}$$

Here $C_\mu = 0.09$, and l is the turbulent length scale. For the sake of consistency the turbulent length has been determined as a function of the hydraulic diameter and is solved for as $l = 0.007 d_h$.

3 Results

3.1 Case 1 RANS simulation

Case 1 was carried out both as a large eddy simulation (LES) and as a k-ω RANS. Several different meshes was used to study the effect of the mesh density on the flow pattern. The two turbulence models resulted in similar flow patterns and therefore only the RANS model will be discussed. An LES simulation will be presented in Case 2. Case 1, which utilized an initial gas velocity (u_g) of 3.24 m/s and liquid velocity (u_l) of 0.87 m/s was run with the interior domain consisting of 77 % gas and 23 % oil at their relative velocities. The interface Courant Number was restricted to 0.3 while the cells with purely one phase in them were restricted to 0.5. The Courant number was used to limit the time step, with the largest allowed time step being 0.005 s. Using these initial conditions and a pressure drop of 110 Pa/m the smooth laminar flow at startup develops into frequent low amplitude waves.

3.1.1 10 m pipe with coarse mesh

Case 1 was first run in a 10 m pipe using a mesh of 672,000 cells using periodic boundary conditions between inlet and outlet as well as symmetry conditions across the centerline (y-axis) while using an interface compression of 1. The mesh information is reiterated in Table 4.

Table 4: Mesh and Pipe Information

Cell dir.	Length (m)	cell size (m)	#.faces
Streamwise	10.0	$6.67{\cdot}110^{-3}$	1500
Outer Dia.	0.1	$5.24{\cdot}110^{-3}$	30
Inner Dia	0.05	$2.62{\cdot}110^{-3}$	30
Annulus	eccentricity=0	$6.72{\cdot}110^{-4}$ to $2.1{\cdot}110^{-3}$	19

The cells in the streamwise direction are spaced 6.67 mm apart evenly throughout the domain. The cells closest to the walls are 0.67 mm thick while the interior region cells are 2.1 mm thick, the near wall region uses a linear progression to merge from the near wall interior region where the cell thickness is constant.

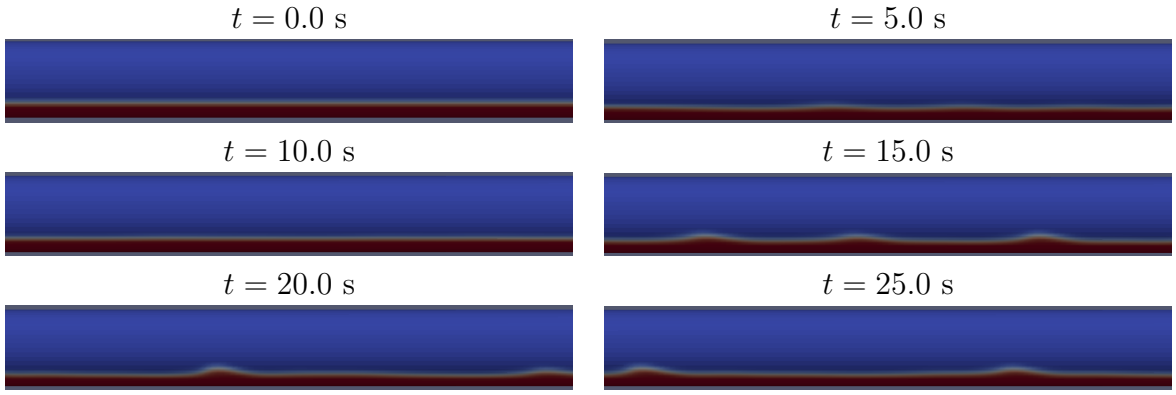

Figure 2: Snapshots of phase field at time intervals of 5 s.

In previous iterations of these flow simulations a startup slug was formed due to poor initial conditions. In the 5 s timestep image if you carefully inspect the central region, there is a small visible buildup of liquid. Because the initial conditions are close to the final result this liquid accumulation does not form the aforementioned slug and significantly reduces the required simulation time. The wave frequency is approximately 4 Hz which resembles that observed during the experiments at IFE. Concerning the wave amplitude it appears that the experimental wave formations have a noticeably larger amplitude than the simulated case. A typical set of waves seen in experiment for this case is shown in Fig.3.

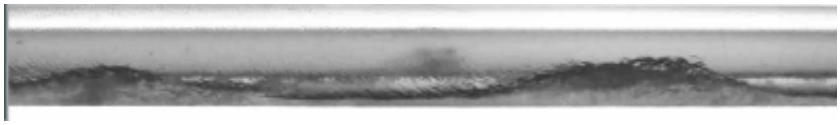

Figure 3: IFE experiment [6]

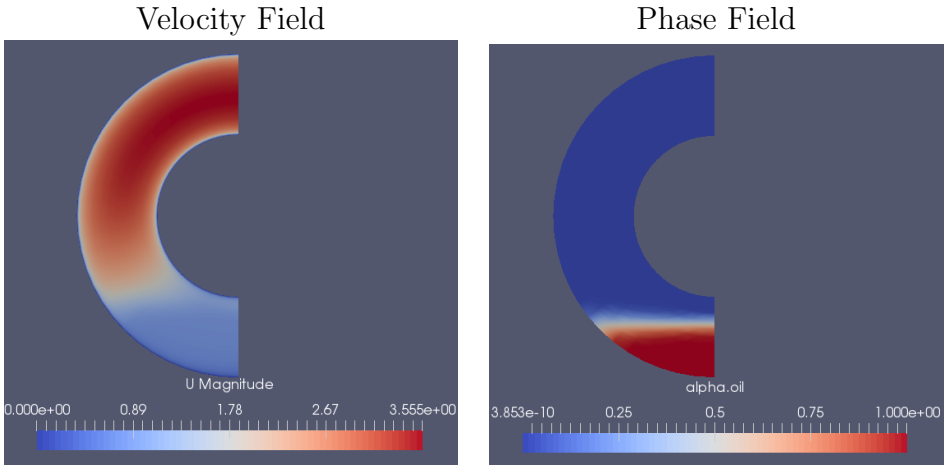

Figure 4: Velocity field and phase fraction distribution at x=5.0 m t=40 s

As seen in Fig.4 the fully developed mean velocity for the gas phase is around 3.0 m/s while the liquid phase is very near the original 0.87 m/s used to initialize the problem. These values match within 10 % of the original magnitudes and indicate that the pressure drop from the experimental results is applicable to this flow regime for pressure driven flow simulations.

3.1.2 3 m pipe with 840 k cells

The second mesh studied in case 1 is significantly refined when compared to the previous iteration and contains 840 k cells distributed along the 3 m pipe. Similarly to the former mesh the pipe is split along the centerline and applied with symmetric boundary conditions to mirror the behavior across the yx-plane.

Table 5: Mesh and Pipe Information

Cell dir.	Length (m)	cell size (m)	#.faces
Streamwise	3.0	$3.33{\cdot}10^{-3}$	900
Outer Dia.	0.1	$5.1{\cdot}10^{-3}$	32
Inner Dia	0.05	$2.55{\cdot}10^{-3}$	32
Annulus	eccentricity=0	$5.37{\cdot}10^{-4}$ to $1.0{\cdot}10^{-3}$	32

The cells along the x-axis (streamwise) of the pipe are a constant 3.33 mm long, while their thickness varies from 0.537 mm close to the wall to 1.0 mm in the central interior region. Along the outer diameter the cells stretch 5.1 mm while along the inner diameter

they are half of that. Compared to the original mesh most of the refinement occurs in the streamwise direction where the number of faces per meter was doubled and in the annulus where the number of faces was increased by 68 %.

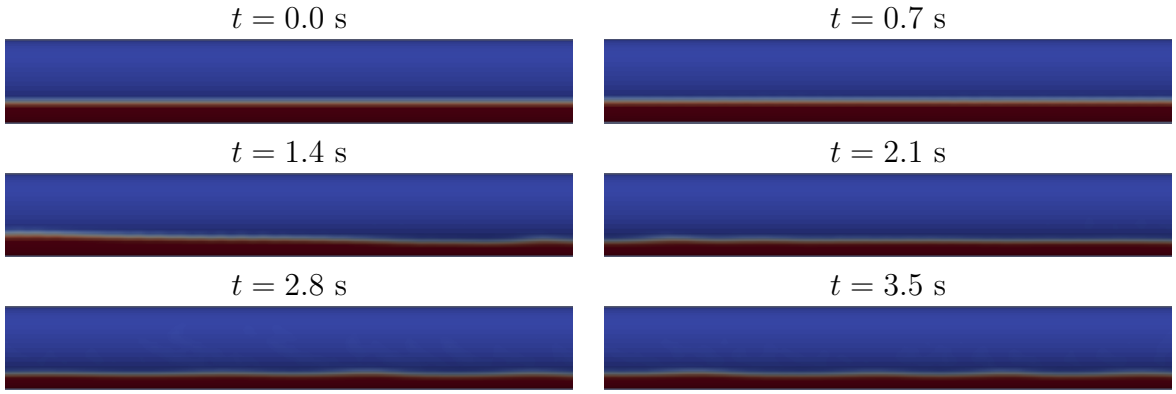

Figure 5: Snapshots of phase field at time steps of 0.7 s

In comparison to the coarse mesh flow regime shown in Fig. 2, the refined pipe flow acts consistent with the coarse mesh behavior. By 2.8 and 3.5 s there are visible oscillations of the surface, these oscillations were seen as a precursor to the formation of larger waves in the coarse mesh where they first occurred at around 10 s. The coarse mesh is a significantly longer pipe which may have an impact on the initial development of the flow when using periodic boundary conditions since the laminar smooth section will stretch further from startup and could explain why oscillations are seen earlier during this sub case.

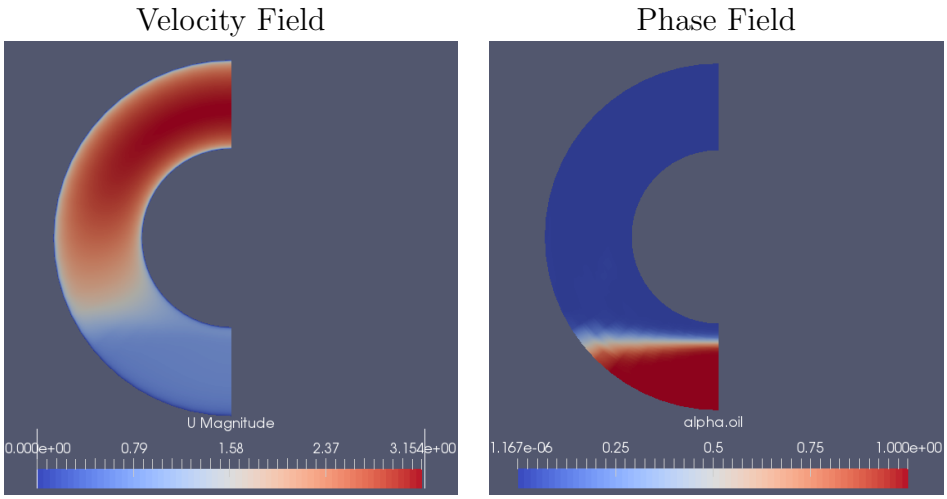

Figure 6: Velocity field and phase fraction distribution at x=1.5 m t=3.5 s

When comparing Fig.6 to Fig.4 it is important to remember that the flow in Fig. 4 is already fully developed wave flow. Fig.6 shows a flow pattern which is still developing, although if the two meshes were to be compared at similar stages the relationship between the two velocity fields remain the same. In the fine mesh both phases are slowed down 11 % when compared to the coarse mesh. The only major difference between the two simulations is that the pipe is shorter with a significantly refined mesh. Further simulation time is required to determine if this decreased velocity experienced will alter the resultant flow regime.

3.2 Case 2 - 2 m Pipe with 1550 k cells

The second case was carried out as a one equation LES simulation, using the Smagorinsky sub grid model. The pipe which is 2 m long and fully concentric consists of 1.55 million cells. The interior domain was initially filled with 38% liquid and 62% gas. At start up the superficial liquid velocity was 0.4 m/s, while the gas phase was travelling at a superficial velocity of 2.0 m/s. A pressure drop of 310 Pa was imposed between the inlet and the outlet of the pipe. As with the remainder of the simulations periodic conditions were used to map the phase distribution and velocity field from the outlet back to the inlet effectively creating an infinite pipe.

Table 6: Mesh and Pipe Information

Cell dir.	Length (m)	cell size (m)	#.faces
Streamwise	2.0	$3.63 \cdot 10^{-3}$	550
Outer Dia.	0.1	$3.98 \cdot 10^{-3}$	80
Inner Dia	0.05	$1.99 \cdot 10^{-3}$	80
Annulus	eccentricity=0	$3.79 \cdot 10^{-4}$ to $8.82 \cdot 10^{-4}$	38

Although further work is needed to determine if the LES simulation solution is converged with respect to mesh size, the mesh described in Fig.6 is the finest used in any of the cases presented in this paper. In the streamwise direction the cells are placed 3.63 mm apart, along the inner diameter the cells are 1.99 mm apart while along the outer diameter they are exactly twice as long. Within the annulus the cells thickness increase by linear progression from 0.379 mm nearest either wall to 0.882 mm in the central region where the width of each cell is held constant.

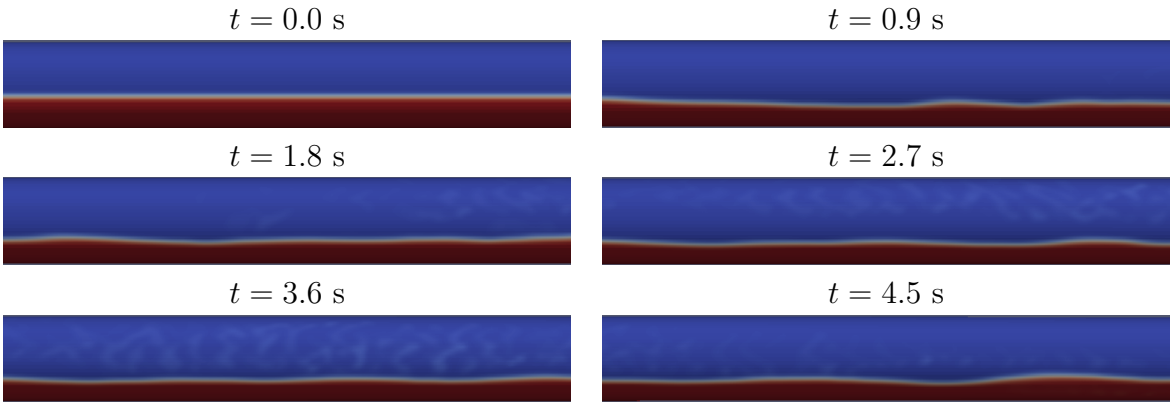

Figure 7: Case 2 flow regime profile

Within the 2m domain of this pipe the flow quickly transitions from smooth stratified flow to wavy flow with distinct waves being visible by 2.7 s. There appears to be some mist like structures throughout the domain especially noticeable at the 3.6 s mark. The turbulent eddies that form in the LES simulation lift and carry these liquid droplets through the domain. As seen in the 4.5 s and 2.7 s image there is less of the mist present, with time it will be possible to determine whether these structures persist throughout the simulation or if it is a passing occurrence related to initialization.

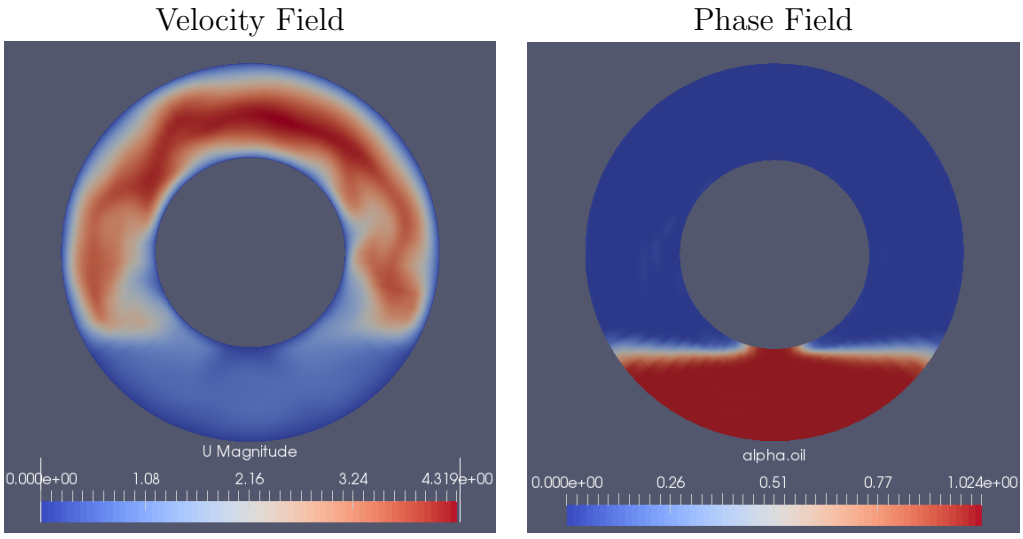

Figure 8: Velocity field and phase fraction distribution $x = 1.5$ m and $t = 4.5$ s

The velocity field distribution and local holdup profile presented in Fig.8 indicate that superficial gas and liquid velocities have deviated in regards to their initial values. At the

given location the liquid holdup is 27%, which yields superficial gas and liquid velocities of 2.36 and 0.29 m/s respectively. When compared to experimental data these flow velocities should generate wavy flow, Fig.3.2 reflects this expected behavior. There are visible patches in the velocity field distribution, these eddy regions seem to closely match the areas where there are liquid droplets in the phase field. Turbulent eddies have been known to lift liquid particles from the surface and transport them through the gas phase which could explain this apparent behavior.

3.3 Case 3, 4 m pipe with 784k cells

Case 3 was simulated in a 4 m pipe with 784 k mesh elements.A symmetric boundary condition was applied along the centerline creating a mirrored boundary about the y-axis. Information about the mesh is summarized in figure 7. The interior was filled with liquid fraction $\alpha_l = 0.43$ and the pressure drop through the domain was set as 1360 Pa. The internal conditions were initialized such such that the superficial gas and liquid velocities was set to 1.85 and 0.65 m/s respectfully. The interface compression coefficient was 0.9.

Table 7: Mesh and Pipe Information

Cell dir.	Length (m)	cell size (m)	#.faces
Streamwise	4.0	$4.0\text{x}10^{-3}$	1000
Outer Dia.	0.1	$5.61{\cdot}10^{-3}$	30
Inner Dia	0.05	$2.80{\cdot}10^{-3}$	30
Annulus	eccentricity=0	$5.3{\cdot}10^{-4}$ to $1.0{\cdot}10^{-3}$	30

The mesh size within the annulus is refined in the near wall region. Using a linear progression the cells adjacent the wall are $0.53\text{x}10^{-4}$ m thick while the largest cell in the refinement region is $0.95\text{x}10^{-4}$ m, these cells border the constant thickness region of the interior where the cells are 1.0 mm wide. The refinement region covers 0.005 m from either wall and thus occupies 40% of the interior space.

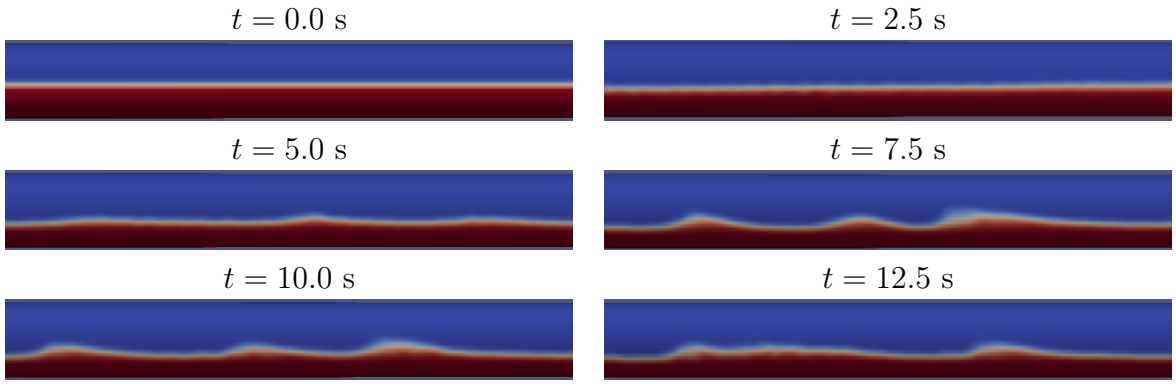

Figure 9: Snapshots of flow regime with 1.5s

The flow quickly develops from smooth stratified to wavy flow. As seen above there appears to be two sets of waves distinguished by their amplitude. The large amplitude waves are seen at t = 7.5 and 10.0 s while the more frequent low amplitude waves are visible at t=5.0, 10.0 and 12.5 s. In both the snapshots at 5.0 and 7.5 s the low amplitude waves are located in between large amplitude waves. When you inspect the 7.5 second image it is noticeable that two of the waves are about to merge and create a larger wave whilst in the 12.5 s snapshot two waves have already come together to generate a significantly longer wave although of low amplitude. Several of these mergers can cause the formation of a large slug. With further simulation time it will be possible to determine if these waves merging lead to the transition from wavy flow to slug flow.

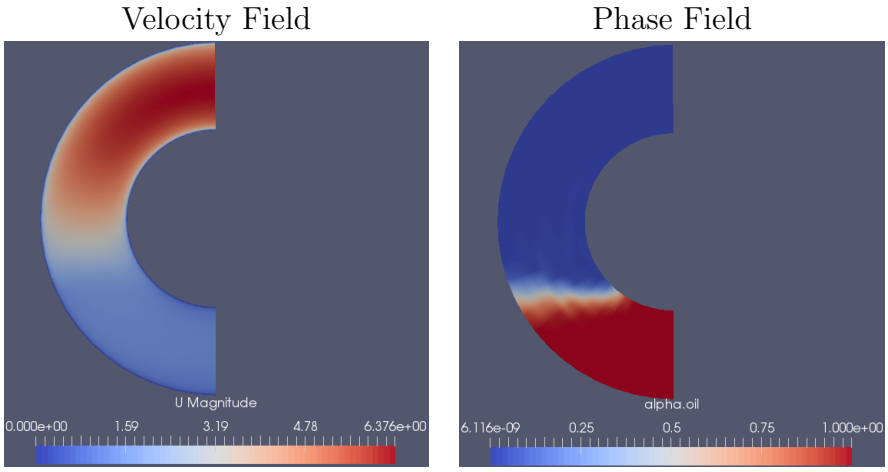

Figure 10: Velocity field and phase fraction distribution x=2 m, t=12.5 s

The velocity profile snapshot indicates that the flow is accelerated from the initial conditions. The superficial gas velocity is approximately 2.73 m/s while the liquid superficial

velocity is 0.8127 m/s, this equates to an increase of around 45 and 25 % respectively when compared to the initialized field. If the flow pattern transitions to slug flow most likely the velocity distribution will drastically change and will have to be reevaluated. Further simulation time and studies are needed to determine if the discrepancy is caused by mesh dependency or if it will be resolved by the transition to slug flow.

3.4 CASE 4, 4 m pipe with 1000 k cells

Using the k-ω RANS model and a 4 m pipe split down the y-plane with a total of 1 million cells case 4 was expected to yield slug flow. The computational domain was initially filled with liquid and gas volume fractions of 0.38 and 0.62 respectively. A pressure drop of 4628 Pa between inlet and outlet was applied while the velocity field was initialized for the two phases as $u_g = 3.0$ m/s and $u_l = 1.2$ m/s

Table 8: Mesh and Pipe Information

Cell dir.	Length (m)	cell size (m)	#.faces
Streamwise	4.0	$3.64{\cdot}10^{-3}$	1100
Outer Dia.	0.1	$5.07{\cdot}10^{-3}$	32
Inner Dia	0.05	$2.53{\cdot}10^{-3}$	32
Annulus	eccentricity=0	$5.34{\cdot}10^{-4}$ to $9.38{\cdot}10^{-4}$	33

As shown above the mesh within the annulus varies, the finest elements are placed near the walls while the central interior region is coarser. The cell closest to the wall is 0.534 mm thick while the widest cell is 0.938 mm. The cells in the streamwise direction are a constant 3.64 mm, while the cells along the outer diameter are 5.07 mm and the inner diameter 2.53 mm.

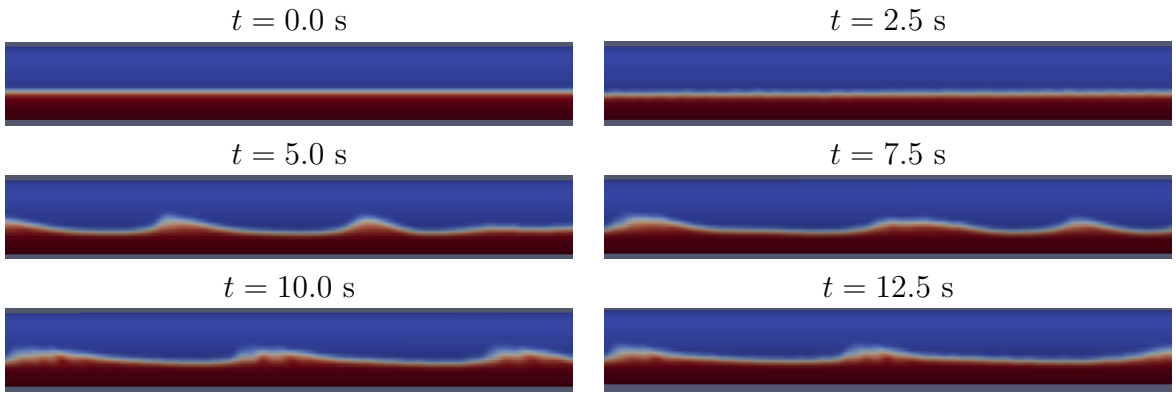

Figure 11: Snapshots of flow regime with timestep 2.5s

As with case 1 and 3 the flow quickly develops from the laminar smooth startup regime to wavy flow. Similarly to case 3 there are indications that waves are combining to produce an increased local liquid holdup, the right hand side of $t = 7.5$ s shows one such case of two waves having merged together. A closer look on the wave interaction beforehand is shown in figure 12.

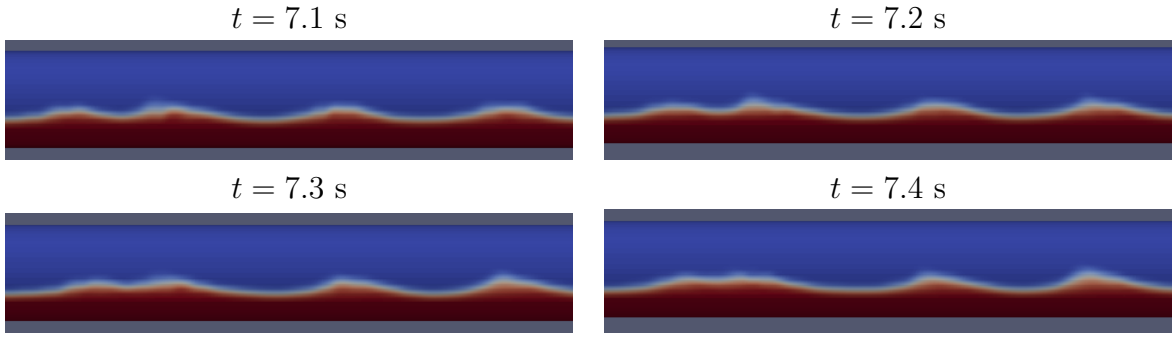

Figure 12: Case 4 Merging Wave

The wave merging seen above takes place just prior to the snapshot at 7.5 s in Fig. 11. The two waves combine to form a local accumulation of liquid. If several of these wave mergers occur it may eventually lead to a situation where the liquid holdup is increased enough to completely fill the cross section of the pipe. A phenomena commonly known as slugging.

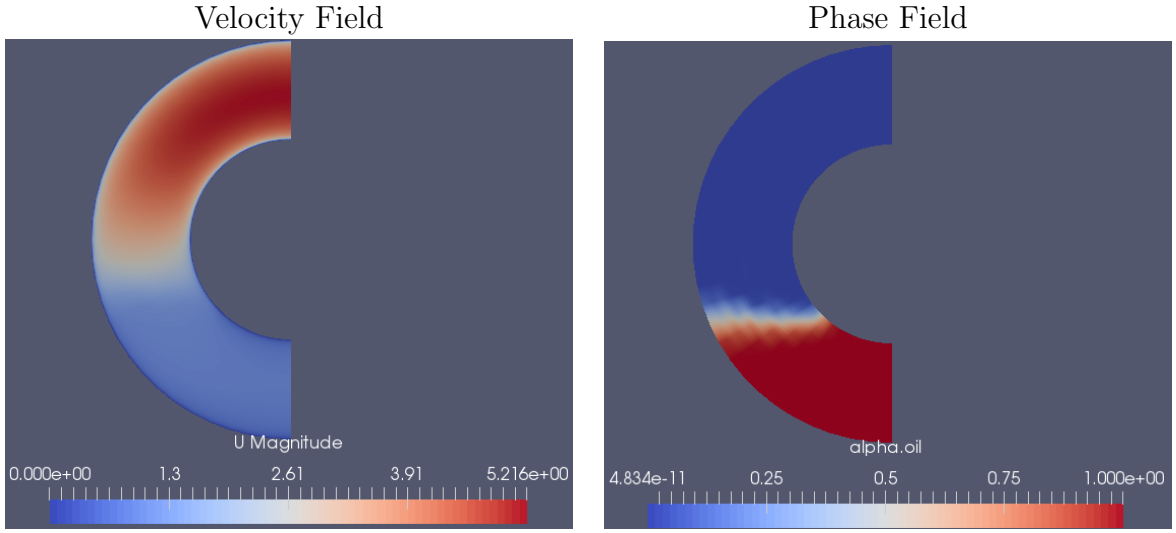

Figure 13: Velocity field and phase fraction distribution at x=1.85 m, t=7.5 s

The cross sectional view shown above was taken directly between two wave peaks, compared to the initial velocity both the liquid and gas phases have experienced a roughly 30% increase to their relative velocities. Similarly to the other cases further work is needed to determine if this discrepancy from experiment is caused by mesh dependencies, experimental setup or other causes.

4 CONCLUSIONS

The four cases studied in this paper yielded wavy flow with indications that transition to slug flow was possible in at least two cases (3,4). Cases 1,3 and 4 were run using a $k-\omega$ RANS formulation while case 2 was simulated using a one equation LES model. All the simulations were carried out using periodic boundary conditions thus mapping the inlet and outlet together. The RANS simulations had a symmetric boundary condition applied about the centerline y-axis reducing the computational domain when compared to the LES simulation. All cases were simulated using the interFoam solver in OpenFOAM and with an applied interface compression coefficient between 0.7 and 1.0

Case 1 resulted in the formation of low amplitude wave flow with liquid holdup up close to the projected result based on experimental data provided by Nossen et.al[6]. Compared to experiment the waves were smaller in amplitude but of similar frequency. Cases 3 and 4 yielded both small and large amplitude waves, in these two cases smaller waves were observed merging together. The waves merging lead to the formation of larger waves and an increase in the local liquid holdup. This behavior is a known precursor to slug flow and with further simulation time it will be possible to determine if these cases will undergo a transition from wavy flow to slug formation.

Early indications point toward a discrepancy with regards to flow pattern and the applied pressure drop across the pipe in comparison to experiment. While the low amplitude high frequency waves reproduce experimental data quite well (Case 1). Cases such as 3 and 4 result in a 30-40% velocity increase in both phases while not yet transitioning to slug flow as the experiments did. It is possible that the increase in the velocity field is exactly because the flow is yet to transition and further work is needed to determine the cause of this disparity. Whether it is simply because it has not transitioned yet or if the discrepancy is caused by the mesh density or other tuning parameters are issues to be investigated in the near future. Analyzing case 1 early results indicate that the mesh density is having an effect on the velocity field and further studies are needed to determine mesh convergence with regards to the final results.

5 ACKNOWLEDGEMENTS

The participants would like to thank the Research Council of Norway, who is funding the project through the PETROMAKS2 program.

REFERENCES

[1] Ali, S. F. and Yeung, H. *Experimental Investigation and Numerical Simulation of Two-Phase Flow in a Large-Diameter Horizontal Flow Line Vertical Riser*. Petroleum Science and Technology (2010) **28** 11

[2] Beggs, D. H. and Brill, J. P. *A study of Two-Phase Flow in Inclined Pipes*. Journal of Petroleum Technology (1973) **25** 05

[3] Caetano, E. F., Shoham, O. and Brill, J. P. *Upward vertical two-phase flow through an annulus* Thesis. The University of Tulsa (1985)

[4] Ekberg, N. P et al *Gas-liquid two-phase flow in narrow horizontal annuli*. Nuclear Engineering and Design (1999) **192** 01:59-80.

[5] Lee, A. H., Sun, J. Y. and Jepson, W.p *Study of Flow Regime Transitions of Oil-Water-Gas Mixtures in Horizontal Pipelines*. Proceedings of the Third (1993) International Offshore and Polar Engineering Conference

[6] Nossen, J. *An experimental study of two-phase flow in horizontal and inclined annuli*. to be published in Introduction to Multiphase 2017 - 'The Cannes Conference'

[7] Peeters, P. T. *CFD of Multiphase Pipe Flow: A Comparison of Solvers* TU Delft Thesis,2016

[8] Petalas, N. and Aziz, K. *A Mechanistic Model for Multiphase Flow in Pipes*. Journal of Canadian Petroleum Technology (2000) **39** 06

[9] Shuard, A. M., Mahmud, H. B. and King, A.j. *Comparison of Two-Phase Pipe Flow in OpenFOAM with a Mechanistic Model* IOP Conference Series: Materials Science and Engineering

[10] Taitel, Y. and Dukler, A. E. *A model for predicting flow regime transitions in horizontal and near horizontal gas-liquid flow*. AIChe Journal (1976) **22** 01

[11] Zhang, H., Wang, Q., Sarica,C. and Brill, J. P. *Unified Model for Gas-Liquid Pipe Flow via Slug Dynamics -Part 1: Model Development* ASME. J. Energy Resour. Technol (2003) **125** 4:266-273